COBEM 2023 27TH INTERNATIONAL CONGRESS OF MECHANICAL ENGENEERING

ABCM Brazilian Society of Mechanical Sciences and Engineering
27th ABCM International Congress of Mechanical Engineering
December 04-08, 2023, Florianópolis-SC, Brazil

COB-2023-0067
THE STUDY OF THE DEVELOPMENT OF AIRCRAFT WAKES NEAR A GROUND PLANE THROUGH A LAGRANGIAN APPROACH

Marília Fernandes Vidille
School of Engineering and Sciences, São Paulo State University (UNESP), Guaratinguetá, SP, Brazil
marilia.f.vidille@unesp.br

Paulo Guimarães de Moraes
Mechanical Engineering Institute, Federal University of Itajubá (UNIFEI), Itajubá, MG, Brazil
pauloguimor@unifei.edu.br

Luiz Antonio Alcântara Pereira
Mechanical Engineering Institute, Federal University of Itajubá (UNIFEI), Itajubá, MG, Brazil
luizantp@unifei.edu.br

Alex Mendonça Bimbato
School of Engineering and Sciences, São Paulo State University (UNESP), Guaratinguetá, SP, Brazil
alex.bimbato@unesp.br

Abstract. *This work uses a Lagrangian method to simulate the behaviour of vortices detached from airplane wings and their interaction with a ground plane. The phenomenon occurs during take-off and landing procedures and may cause accidents in airports. The lagrangian computational technique used is the discrete vortex method, whereby the vorticity field is represented by Lamb discrete vortex, whose objective is to solve the vorticity transport equation, obtained from the Navier-Stokes and continuity equations. To reduce the complexity of the solution, the viscous splitting algorithm is used, which simulates the advection and diffusion processes separately, but at the same time step of the numerical simulation. To simulate the diffusion, the random walk method is used. According to this method, random numbers are generated to count the radial and circumferential displacements of the discrete particles. To simulate the advection, it is necessary to know the velocity field in the position occupied by each Lamb discrete vortex and it is composed of three parcels: the incident flow, the solid boundary and the discrete vortex cloud contributions. The solid boundary is represented by a source panel method to satisfy the impermeability boundary condition and a discrete vortex is positioned in the neighbourhood of each panel, at each time step of the numerical simulation, to satisfy the no-slip condition. The vortex-vortex interaction is the more onerous part of the velocity field calculation, because its computational costs, using the Biot-Savart law, are proportional to* Z^2*, where Z is the number of particles in the computational domain. The increase in the number of particles because of the vorticity generation makes the CPU time high and the simulation prohibitive. Therefore, an accelerator algorithm based on the fast multipole method is implemented to avoid this. The principle of this algorithm is to divide the computational domain into square boxes to enable more interactions among boxes than interactions among particles. The numerical results are compared with experimental ones and show that the use of the fast multipole method makes the simulations viable, well reproducing the vortices trajectory, even when the vorticity field is discretized using a large number of vortex particles.*

Keywords: *aircraft wakes, accelerator algorithm, fast multipole method, panel method, lagrangian description*

1. INTRODUCTION

The development of the aeronautic industry is one of the tools for making the planet globalized. Without it, it is impossible to have international relations. It is necessary to develop many areas of research because of the high demand on this industry. One of these areas is the Fluid Mechanics, which is a science that studies, among other things, the effect of forces in fluid flows.

The domain of this science is essential to the security and competitiveness of the aeronautic industry, whereby it is possible to use the resources optimally. The air traffic became very intense in the last decades, which makes the accumulation of airplanes for take-off and landing procedures, almost simultaneously very often in different airports around the world.

To realize the take-off and landing procedures in the shortest time possible, keeping security, it is necessary to evaluate the behavior of vortex structures detached from airplane wings, ensuring that there is enough time to dissipate these structures before another airplane uses the track. The generation of vorticity from an airplane´s wings is a phenomenon

that changes the flow velocity field. It can cause serious accidents to a second aircraft that will operate on the same track several minutes after the first pass. The first requirement for air traffic control at airports is preventing an aircraft from operating in the wake of another (Machol, 1993).

The main objective of the present research is to perform simulations about the behavior of vortices detached from airplane wings near the ground, specially because of the importance of this physical situation.

To simulate physical situation, it is possible to use Eulerian or Lagrangian description. The Eulerian description uses a mesh to discretize the domain, which causes computational efforts and can cause problems in formulating boundary conditions if the problem has a complex geometry; the use of the Lagrangian description avoid these problems.

The Lagrangian approach is characterized by the discretization of a flow property, the vorticity, in this case, as a set of particles, that are individually followed in their trajectories on the fluid domain and the properties are calculated only in function of the time. The main Lagrangian method is the Discrete Vortex Method, whereby the discretized property is the vorticity (Chorin, 1973; Lewis, 1999; Alcântara Pereira *et al*., 2004; Bimbato *et al*., 2018).

According to the Discrete Vortex Method, the numerical simulation of the evolution of the vorticity field in time is realized using a cloud of Lamb discrete vortex. To make the simulation feasible, it is possible to divide the solution into two processes: the advection and the diffusion, according to the viscous splitting algorithm, proposed by Chorin (1973).

The viscous splitting algorithm allows to solve the diffusion and the advection separately but at the same time step of the numerical simulation. To solve the advection, it is necessary to calculate, at each time step, the velocity field of the flow at each discrete vortex. This calculation is composed of three influences: solid boundary (airport track), incident flow (in the case of this work, this influence is not considered) and the vortex-vortex interaction, where each discrete vortex induces velocity in all the other ones. It is important to mention that it is necessary Z^2 operations to each Z discrete vortices present in the computational domain when the Biot-Savart law (BS) is used to compute the vortex-vortex interaction.

To reduce the computational time of the vortex-vortex interaction, the fast multipole method (FMM) is implemented (Greengard and Rokhlin, 1987; Nishimura, 2002; Ricciardi, 2016; Ricciardi *et al*., 2017a; Ricciardi *et al*., 2017b). According to this method, the computational domain is divided into square boxes, thus, a cluster of particles is formed from particles that are placed into a box. The principle is to compute, mostly, interactions among clusters of particles that are far from each other, instead of computing all the vortex-vortex interactions. The Biot-Savart law is not completely abandoned, since it is used to compute the vortex-vortex interactions among particles that are inside the same box or among particles that are placed in nearby boxes. The FMM is listed as one of the top 10 algorithms of the twentieth century (Cipra, 2000).

To solve the diffusion equation, several methods have been proposed. The authors believe that, in the case of the present paper, the most appropriate one is the random walk method, proposed by Chorin (1973) and modified by Lewis (1991). In this method, the diffusion is simulated using random numbers to compute the radial and circumferential displacements of the discrete vortices. Since it is a probabilistic method, its accuracy is not high, and its use is restricted to situations where the Reynolds number is high, as in the preset work. Finally, it is important to mention that the simulations performed in this work do not use any turbulence modelling, considering just the macro-scale phenomena.

2. GOVERNING EQUATIONS

The counterrotating pair of vortices detached from airplane wings is showed in Figure 1, whereby the pair of vortices is represented by Z Lamb discrete vortices with a gaussian distribution of vorticity and the circulation of vortex clouds, $+\Gamma^*$ and $-\Gamma^*$, are related to the lift force, F_L, according to the Kutta-Joukowsky law, as in Eq. (1). The pair of vortices is detached from a height of h^*, the airplane wingspan is b^*, the solid boundary is S_1. And, this case, is the track of the airport, whose length is x^*_{track}.

$$\Gamma^* = \frac{F_L}{\rho u^* b^*} \tag{1}$$

The fluid density and the fluid velocity are represented by ρ and u^*, respectively, in Eq. (1).

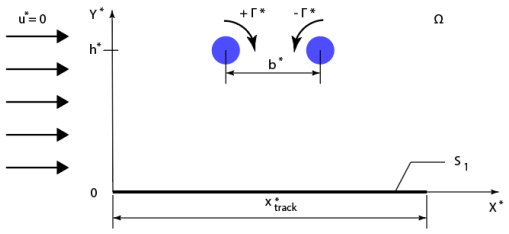

Figure 1. The model used in the numerical simulation.

The principle of mass conservation and the principle of momentum conservation govern the problem and are written in the forms of the continuity equation (Eq. 2) and the Navier-Stokes equations (Eq. 3). The continuity and the Navier-Stokes (N-S) equations, according to Eq. (2) and Eq. (3), respectively, are responsible for the dimensional region, Ω.

$$\boldsymbol{\nabla}^* \cdot \boldsymbol{u}^* = 0 \tag{2}$$

$$\frac{\partial \boldsymbol{u}^*}{\partial t^*} + (\boldsymbol{u}^* \cdot \boldsymbol{\nabla}^*)\boldsymbol{u}^* = -\frac{1}{\rho}\boldsymbol{\nabla}^* p^* + \nu \nabla^{*2}\boldsymbol{u}^* \tag{3}$$

The velocity vector field, the pressure field and the fluid kinematic viscosity coefficient are represented by $\boldsymbol{u}^*$, p^* and ν, respectively, in Eqs. (2) and (3).

The impermeability and the non-slip conditions must be satisfied on S_1. In accordance with these boundary conditions, the normal ($u_n{}^*$) and the tangential ($u_t{}^*$) velocity components of a fluid particle must be equal to the normal ($v_n{}^*$) and the tangential ($v_t{}^*$) velocity components of the boundary, respectively; (see Eqs. (4) and (5)).

$$u_n{}^* - v_n{}^* = 0 \tag{4}$$

$$u_t{}^* - v_t{}^* = 0 \tag{5}$$

In order to make the problem non-dimensional, the following characteristic quantities are used: b^*, characteristic length and Γ^*/b^*, characteristic velocity. Thus, the continuity and the Navier-Stokes equations become:

$$\boldsymbol{\nabla} \cdot \boldsymbol{u} = 0 \tag{6}$$

$$\frac{\partial \boldsymbol{u}}{\partial t} + (\boldsymbol{u} \cdot \boldsymbol{\nabla})\boldsymbol{u} = -\boldsymbol{\nabla} p + \frac{1}{Re}\nabla^2 \boldsymbol{u} \tag{7}$$

In Eq. (7), *Re* is the Reynolds number, which is defined as:

$$Re = \frac{\Gamma}{\upsilon} \tag{8}$$

The impermeability and the non-slip conditions become, respectively:

$$u_n - v_n = 0 \tag{9}$$

$$u_t - v_t = 0 \tag{10}$$

The vorticity transport equation is obtained taking the curl of Eq. (7) and using Eq. (6). This procedure eliminates the pressure term of the vorticity equation, whose two-dimensional form is (Batchelor, 1967):

$$\frac{\partial \omega}{\partial t} + (\boldsymbol{u} \cdot \boldsymbol{\nabla})\omega = \frac{1}{Re}\nabla^2 \omega \tag{11}$$

In Eq. (11), ω is the only non-zero component of the vorticity vector, $\partial\omega/\partial t$ represents the local vorticity variation rate, $(\boldsymbol{u} \cdot \boldsymbol{\nabla})\omega$ represents the advective vorticity variation rate and $\nabla^2\omega/Re$ is the diffusive vorticity variation rate. Since the simulations are realized through a lagrangian description, it is not necessary to deal with the non-linear term represented by $(\boldsymbol{u} \cdot \boldsymbol{\nabla})\omega$ (see Section 3).

3. SOLUTION METHOD

To solve the problem studied in this work, it is necessary to use the viscous splitting algorithm, proposed by Chorin, (1973), whereby it is possible to simulate the advection (Eq. 12) and diffusion (Eq. 13) processes separately, but at the same time step of the numerical simulation.

$$\frac{\partial \omega}{\partial t} + (\boldsymbol{u} \cdot \boldsymbol{\nabla})\omega = \frac{D\omega}{Dt} = 0 \tag{12}$$

$$\frac{\partial \omega}{\partial t} = \frac{1}{Re}\nabla^2 \omega \tag{13}$$

The material derivate, present in Eq. (12) and responsible for compute the advection effects, makes evident the lagrangian characteristic of the solution method.

To follow the trajectory of each particle, present in the domain, it is necessary to solve Eq. (14).

$$\frac{d\boldsymbol{x}}{dt} = \boldsymbol{u}(\boldsymbol{x}, t) \tag{14}$$

It is possible to note that, to solve Eq. (14), it is necessary to know the velocity field in the position occupied by each Lamb discrete vortex used to represent the vorticity present in the fluid domain. Then, the equation of the vorticity trajectory is solved for each discrete vortex present in the domain.

In this paper, the velocity field is composed of the velocity induced by the track (see Section 3.1) and of the velocity induced by the vorticity field (see Section 3.3).

3.1 Solid boundary contribuition: the Panel Method

The body surface is discretized by flat panels over which singularities are distributed. The singularities intensities are calculated to annulate the normal velocity in the pivotal point at each flat panel. The solid boundary present in the proposed problem is the airport track, which is an open contour, whereby it is used the Neumann's boundary condition.

The singularities used are of source type, constantly distributed, according to Figure 2(a). The u and v components, showed in the Figure 2(b), of the velocity induced for the constantly source type distribution, $\sigma(x)$, of a flat panel at a point P, located near the panel are, respectively (Katz and Plotkin, 1991):

$$u = \frac{\sigma(x)}{2\pi} ln \frac{r_1}{r_2} \tag{15}$$

$$v = \frac{\sigma(x)}{2\pi} (\theta_2 - \theta_1) \tag{16}$$

Whereby $r_1 = \sqrt{(x - x_1)^2 + y^2}$, $r_2 = \sqrt{(x - x_2)^2 + y^2}$, $\theta_1 = \text{tg}^{-1}[y/(x - x_1)]$ and $\theta_2 = \text{tg}^{-1}[y/(x - x_2)]$.

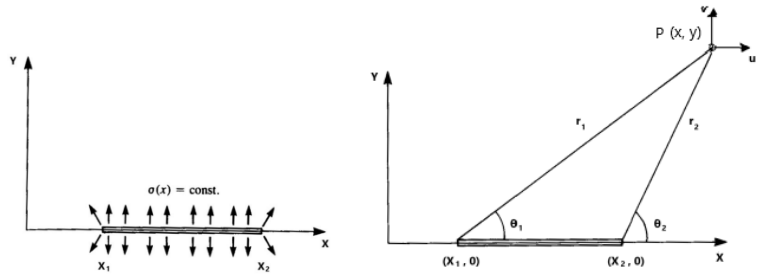

Figure 2. (a) Singularity distribution over a flat panel. (b) Components of the velocity induced at a point *P*. Adapted from Katz and Plotkin (1991).

The impenetrability condition (Eq. 9) is obtained by the decomposition in the normal direction of the u and v components of the velocity induced at the pivotal point of each panel and imposing that the summatory of these components must be zero in the normal direction. Then, an algebraic system of equations must be solved to determine the values of σ that should be distributed on each flat panel to ensure the impermeability condition in the normal direction. Then, an algebraic system of equations must be solved to determine the values of σ that should be distributed on each flat panel to ensure the impermeability condition.

3.2 Vorticity generation

The fluid flow around a solid boundary causes the boundary layer formation, because of the non-slip condition, represented by Eq. (10). Due to the boundary layer formation, the vorticity generation phenomenon occurs, including the rotation of the fluid particles and in some situations, the flow separation.

In order to numerically represent the physical situation previously described, in the problem proposed in this work, the vorticity is generated at each time step of the simulation to annul the tangential component of the velocity vector at each pivotal point of the panels used to discretize the airport track, satisfying Eq. (10). To do this, an algebraic system of

equations must be solved to determine the intensity (Γ) of each nascent discrete vortex necessary to annulate the tangential velocity component induced by the solid boundary (Eqs. 15 and 16) and by the vortex cloud at the pivotal point of each panel (Eqs. 17 and 18), satisfying the no-slip condition and the circulation conservation law (Eq. 19).

$$u_{ij} = \frac{\Gamma_j(y_i - y_j)}{2\pi {r_{ij}}^2}\left[1 - exp\left(-5{,}02572\frac{{r_{ij}}^2}{{\sigma_{0j}}^2}\right)\right] \tag{17}$$

$$v_{ij} = \frac{-\Gamma_j(x_i - x_j)}{2\pi {r_{ij}}^2}\left[1 - exp\left(-5{,}02572\frac{{r_{ij}}^2}{{\sigma_{0j}}^2}\right)\right] \tag{18}$$

$$\sum_{i=1}^{M} \Gamma_i = 0 \tag{19}$$

In Eqs. (17-19), u_{ij} and v_{ij} are the tangential velocity components induced by discrete vortex j at the pivotal point i, $r_{ij} = \sqrt{(x_i - x_j)^2 + (y_i - y_j)^2}$ is the module of the distance between them and M is the number of flat panels used to represent the airport track.

As an example, Figure 3 shows the process of vorticity generation considering the track discretized into four flat panels, whereby co_1, co_2, co_3, co_4 are the pivotal points, $pshed_1$, $pshed_2$, $pshed_3$, $pshed_4$ are the shedding points of discrete vortices and *eps* is the distance of vorticity generation , which is equal to the core radius of Lamb discrete vortex, σ_0 (Alcântara Pereira, 1999).

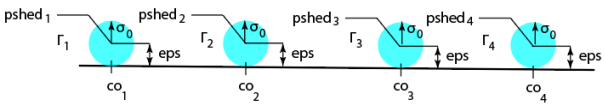

Figure 3. Vorticity generation at the surface of the airport track discretized into four flat panels.

3.3 Vortex-vortex contribuition

There are two forms to calculate the vortex-vortex interaction in this work: through the Biot-Savart law or through the fast multipole method. When it is used the Biot-Savart law, it is necessary Z^2 operations to each Z discrete vortices present in computational domain, but using the fast multipole method, it is necessary $Z \log Z$ or, in the best case, Z operations to each Z discrete vortices present in the domain (Koumoutsakos, 1993).

To avoid the use of the Biot-Savart law, which is a heavy limitation on lagrangian methods, the fast multipole method, previously implemented by Vidille *et al.* (2022) is used in this work. The main idea of this algorithm is clustering the influence of elements close to each other into multipole expansions and evaluate their interactions at distant locations. If the method is correctly used, the computational time is reduced, when it is compared to the computational time necessary to compute the velocity field using only the Biot-Savart law.

It is necessary to pass through a pre-processing step, whereby the computational domain is divided into 4^L square boxes (L is the maximum refinement level) to cluster the influence of particles (discrete vortices) close to each other into multipole expansions, because the mechanism for time reduction is to promote more interactions among square boxes than interactions among particles. Then, after divide the domain in square boxes, lists of neighbors boxes and well-separated boxes are created. Considering two boxes, B and b, whereby b is a child box of B, B can have up to 9 boxes sharing a node, being 8 neighbors boxes and B itself. Each one of these 9 boxes have 4 child boxes, totaling 36 children box, which can be classified as b itself, the near neighbors of b (8 boxes) and the 27 well-separated boxes in the interaction list of b. After classifying the boxes, the particles are mapped to determine in which box they are at the maximum refinement level.

Then, when the pre-processing step is finished, there are some steps of the fast multipole method that need to be performed. The first step is called particle-to-multipole and consists of creating multipole expansion a, in the center of the box b, in the finest level L, using a Taylor's series truncated after p terms, for Z discrete vortex with intensity Γ_i, with a complex distance of z_i from the center of the box, represented by Eq. (20). The sum of all vortex particle intensities is given by Eq. (21).

$$a(b,k,L) = \sum_{i=1}^{Z} -\Gamma_i \frac{{z_i}^k}{k} \tag{20}$$

$$Q(L) = \sum_{i=1}^{Z} \Gamma_i \tag{21}$$

The second step is called multipole-to-multipole and consists of passing the influences from the center of the children box, *b*, to the center of the parent box, *B*, at level *l-1*, resulting in $a(B,k,l-1)$, according to Eq. (22). The intensity of the multipoles in level *l-1*, $Q(l-1)$, is the sum of the children's intensities, $Q(l)$, according to Eq. (23).

$$a(B,k,l-1) = \sum_{i=1}^{4} \left\{ \left[\sum_{kk=1}^{k} a_i(kk,l) {z_i}^{k-kk} \binom{k-1}{kk-1} \right] - \left[Q_i(l) \frac{{z_i}^k}{k} \right] \right\} \tag{22}$$

$$Q(l-1) = \sum_{i=1}^{4} Q_i(l) \tag{23}$$

The step whereby the interactions among boxes occur is the multipole-to-multipole which is made up to level 2 because it is the first level that has boxes far enough apart. The interaction list of a box *b* contains, at most, 27 boxes *j* that interact via multipole-to-local with objective box *B*, resulting in the multipole-to-local variable $b(B,kk,l)$. The variable called *nbox* is used to represent the non-empty boxes that are included in the interaction list of *B*, z_j is the complex distance between the box of interest and the box from the interaction list and the variables *a* and *Q* are calculated in the particle-to-multipole and multipole-to-multipole steps.

$$b(B,kk,l) = \sum_{j=1}^{nbox} \left[\frac{a_j(k.l) \left(\frac{-1}{z_j}\right)^k \binom{kk+k-1}{kk-1}}{{z_j}^{kk}} - \frac{Q_j(l)}{kk {z_j}^{kk}} \right] \tag{24}$$

The next step is very similar to the multipole-to-multipole, but here, the influence is passed from *B* to a child box, *b*. This step is called local-to-local and Eq. (25) calculates the local-to-local influence in a box in the level *l+1* from its parent at level *l*; *b(k,l)* is the local representation of the far field multipole expansions at the parent box and z_j is the complex distance between the parent's and the children's centers.

$$c(b,k,l+1) = \sum_{i=1}^{4} \left\{ \sum_{kk=k}^{p} \left[b(k,1)(-z_i)^{kk-k} \binom{kk}{k} \right] \right\} \tag{25}$$

The last step can be divided into two: local-to-particle and particle-to-particle. The local-to-particle consists of doing the reverse process of the particle-to-multipole; in other words, one transfers the influence from the center of a box to all particles within the box through another Taylor's series, showed in Eq. (26), whereby ${vv_i}^w$ is the vortex-vortex interaction, *b(l)* is the sum of multipole-to-multipole and local-to-local steps in a box from the highest refinement level (*l*) and z_i is the complex distance between the discrete vortex *i* and the center of its box.

$${uv_i}^w = {vv_i}^w + \sum_{k=1}^{p} b(k,1) k {z_i}^{k-1}, w = 1,2 \text{ and } i = 1,Z \tag{26}$$

The particle-to-particle consists on the interaction between particles of the same box and on the interaction between particles from boxes in the neighbor list through the Biot-Savart law, which is done using the Eq. (27), where Γ_j is the intensity of the *j* vortex and $c_{ij}^n[\boldsymbol{x}_i(t) - \boldsymbol{x}_j(t)]$ is the $n-th$ component of the induced velocity at a discrete vortex *i* by a discrete vortex *j*.

$${vv_i}^w(\boldsymbol{x}_i,t) = \sum_{j=1}^{Z} \Gamma_j c_{ij}^w[\boldsymbol{x}_i(t) - \boldsymbol{x}_j(t)], w = 1,2 \text{ and } i = 1,Z \tag{27}$$

Since the velocity field in the position occupied by each discrete vortex is determined, it is necessary to impose a dislocation to each vortex particle present in the domain through a first order Euler scheme, according to the Eq. (28), whereby ς_i is the random walk displacement, which is given by random walk method (Lewis, 1999) – see Eq. (29).

$$x_i(t + \Delta t) = x_i(t) + uv_i^w(t)\Delta t + \varsigma_i, w = 1, 2 \text{ and } i = 1, Z \tag{28}$$

$$\varsigma_i = \sqrt{\frac{4\Delta t}{Re} ln\left(\frac{1}{P}\right)} [cos(2\pi Q) + \Psi\, sin(2\pi Q)] \tag{29}$$

In Eq. (29), $\Psi = \sqrt{-1}$, P and Q are random numbers between 0 and 1.

4. RESULTS

In order to evaluate the use of the accelerate algorithm of the fast multipole method, two identical vortex clouds, composed by *nz* discrete vortices with intensity $\pm 1/nz$, are positioned, as shown in Figure 1, to simulate the vortex cloud detached from airplane wings during a landing or a take-off procedure, near the ground, that was discretized into *M* flat panels, according to the panel method (Katz and Plotkin, 1991).

The vortex clouds are created using a diffusion dislocation through the generation of random numbers, then, the *nz* vortex are initially positioned on the origin of the reference system and they are randomly distributed until the more distant discrete vortex reach a distance equal to $0.1b^*$, according to Figure 1. Using this approach, it is possible to ensure a gaussian distribution of the vorticity contained in the clouds as if it were a big Lamb vortex.

There are performed seven situations: the first is the simulation that the vortex-vortex interaction is made using only the Biot-Savart law; then, six simulations using the fast multipole method to compute the vortex-vortex interaction are performed, changing the parameters of the refinement levels and the step of the simulation that the fast multipole method starts to be used. All of these simulations that the fast multipole method is used starts computing the vortex-vortex interaction through the Biot-Savart law and, when the population of discrete vortices in the domain reaches a considerable value, the accelerator algorithm is used. This approach is used to reduce the numerical error intrinsic to the use of the accelerator algorithm.

The common numerical parameters used in these simulations are: $Re = 7.65 \times 10^3$, $nz = 2.5 \times 10^4$, $M = 500$, $\Delta t = 0.05$; the simulations are performed until $t = 110$. In the simulations whereby the FMM algorithm is considered, the number of terms used on the Taylor series (p) is equal to 25 Vidille et al. (2022) and the refinement level is called by L. In short, the simulations carried out used: (i) only the Biot-Savart law; (ii) the Biot-Savart law until $t = 10$, then, the FMM algorithm with $L = 6$ until the end of the simulation; (iii) the Biot-Savart law until $t = 10$, then, the FMM algorithm with $L = 7$ until the end of the simulation; (iv) the Biot-Savart law until $t = 10$, then, the FMM algorithm with $L = 8$ until the end of the simulation; (v) the Biot-Savart law until $t = 10$, then, the FMM algorithm with $L = 6$ until $t = 20$, $L = 7$ until $t = 40$ and $L = 8$ until the end of the simulation; (vi) the Biot-Savart law until $t = 10$, then, the FMM algorithm with $L = 6$ until $t = 30$, $L = 7$ until $t = 50$ and $L = 8$ until the end of the simulation; (vii) the Biot-Savart law until $t = 20$, then, the FMM algorithm with $L = 6$ until $t = 30$, $L = 7$ until $t = 40$ and $L = 8$ until the end of the simulation.

Because of the vorticity generation, the number of discrete vortices in the domain increases. The number of discrete vortices in the beginning of the simulations is $Z = 5.0 \times 10^4$ and, in the end of the simulations, is $Z = 1.15 \times 10^6$. The computational time dispended in all the simulations is shown in Table 1.

Table 1. Computational time dispended in the numerical simulations.

Simulations	Computational time (days)
(i)	26.95
(ii)	3.55
(iii)	1.96
(iv)	2.03
(v)	1.70
(vi)	2.39
(vii)	1.92

According to Table 1, using the fast multipole method in the simulations decreases the computational time. The simulation (*i*) uses only the Biot-Savart law to calculate the vortex-vortex interaction and it is possible to see that its computational time is very high, making the simulation almost unfeasible. The simulations (*ii*), (*iii*) and (*iv*) use the fast multipole method starting when $t = 10$ and the refinement level is $L = 6$, $L = 7$ and $L = 8$, respectively, until $t = 110$. The expect, in these cases, is that the computational time decreases when higher refinement levels are used. The simulation that $L = 6$ (ii) has a higher computational time than the simulations whereby $L = 7$ and $L = 8$, but the simulation whereby $L = 7$ (iii) has a lower computational time than the simulation whereby $L = 8$ (iv), contrary to what is expected at first. That situation may occur when the number of discrete vortices present in the domain is not high

enough to use a higher refinement level. Then, the refinement level $L = 8$ is too high to be used from $t = 10$ until the end of the simulation.

The difference between the simulations (v) and (vi) is the range of use of the refinement levels. In the simulation (v), the range is lower than in the simulation (vi); in other words, the higher levels, in simulation (vi) start to be used later than in the simulation (v), what makes the ratio between the number of particles in the computational domain and the number of squares in the maximum refinement level ($Z/4^L$) higher in the simulation (vi). It is because of this that the computational time in simulation (vi) is higher than in (v). The simulation (vii) is different because of the moment that the fast multipole method starts to be used. The fast multipole method starts to be used when $t = 20$, later than the other simulations that use the accelerator algorithm and the range of use of the refinement levels is lower than the one used in other simulations, what makes the use of the higher refinement levels greater than the simulation (vi) and the computational time lower. Again, in the simulation (vii), the ratio between the number of particles in the computational domain and the number of squares in the maximum refinement level ($Z/4^L$) is higher and for longer than in the others.

In Figure (4) is shown the trajectories of right-side vortex cloud. The numerical results obtained are compared to the experimental conducted by Zheng and Ash[1] (1996, apud Liu and Srnsky, 1990). Figure 4(a) shows the comparation of the right side of the discrete vortices cloud, obtained using only the Biot-Savart law (simulation i) and the experimental results, to validate the use of this algorithm. It is possible to observe, in Figure 4(b), how the FMM algorithm presents bad results when the number of particles in the computational domain is not great enough and the fast multipole method starts to be used earlier, what makes the ratio $Z/4^L$ lower; in these situations, the numerical error in the velocity field computation is too high. The best result is the one that comes closest to the result obtained in the simulation that the vortex-vortex interaction is calculated only through the Biot-Savart law (i).

Figure 4(c) shows the best result of the simulations that the fast multipole method is used (simulation vii), again, it is important to mention that this simulation has the higher ratio $Z/4^L$, turning the numerical error in the velocity field and, consequently, in the trajectory of the right side of the discrete vortices cloud lower.

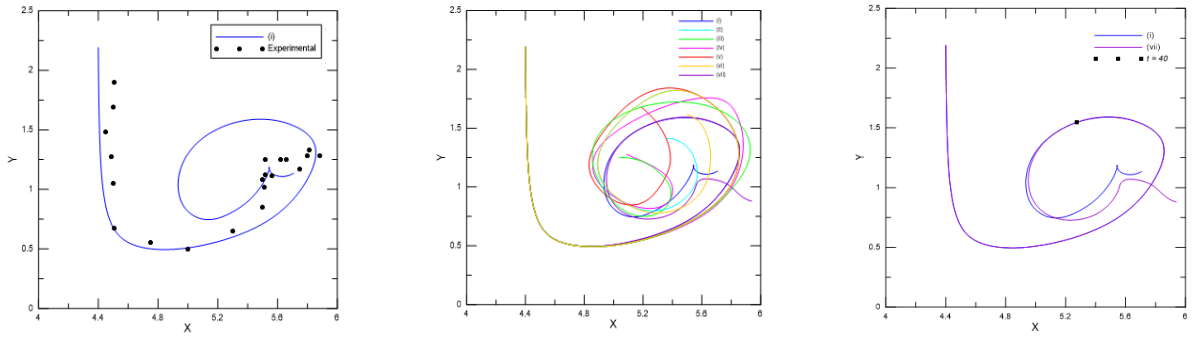

(a) (b) (c)

Figure 4. Comparison between the simulations presented and the experimental results of the right side of the discrete vortices cloud.

Figure 4(c) shows the moment whereby the simulation (vii) starts to diverge from the simulation (i) using a black point. This moment is $t = 40$, when the refinement level starts to be $L = 8$ and the amount of discrete vortices in the domain is $Z = 4.5 \times 10^5$.

The Figure 5 shows the vorticity field of the simulation that has the best result (simulation vii), divided in six time steps: (a) $t = 0.05$; (b) $t = 22.5$; (c) $t = 45$; (d) $t = 67.5$; (e) $t = 90$; (f) $t = 110$. It is possible to see that the right and the left sides of the discrete vortices cloud are not mirrored, because of the use of the random walk method to simulate the diffusion of the vorticity. Since this method is not deterministic, there are generated random values to compute the radial and circumferential displacements, what causes this difference between the left and right sides.

[1] Liu, H.T. and Srnsky, R.A., 1990. "Laboratory investigation of atmospheric effects on vortex wakes". *Flow Research, Inc.*.

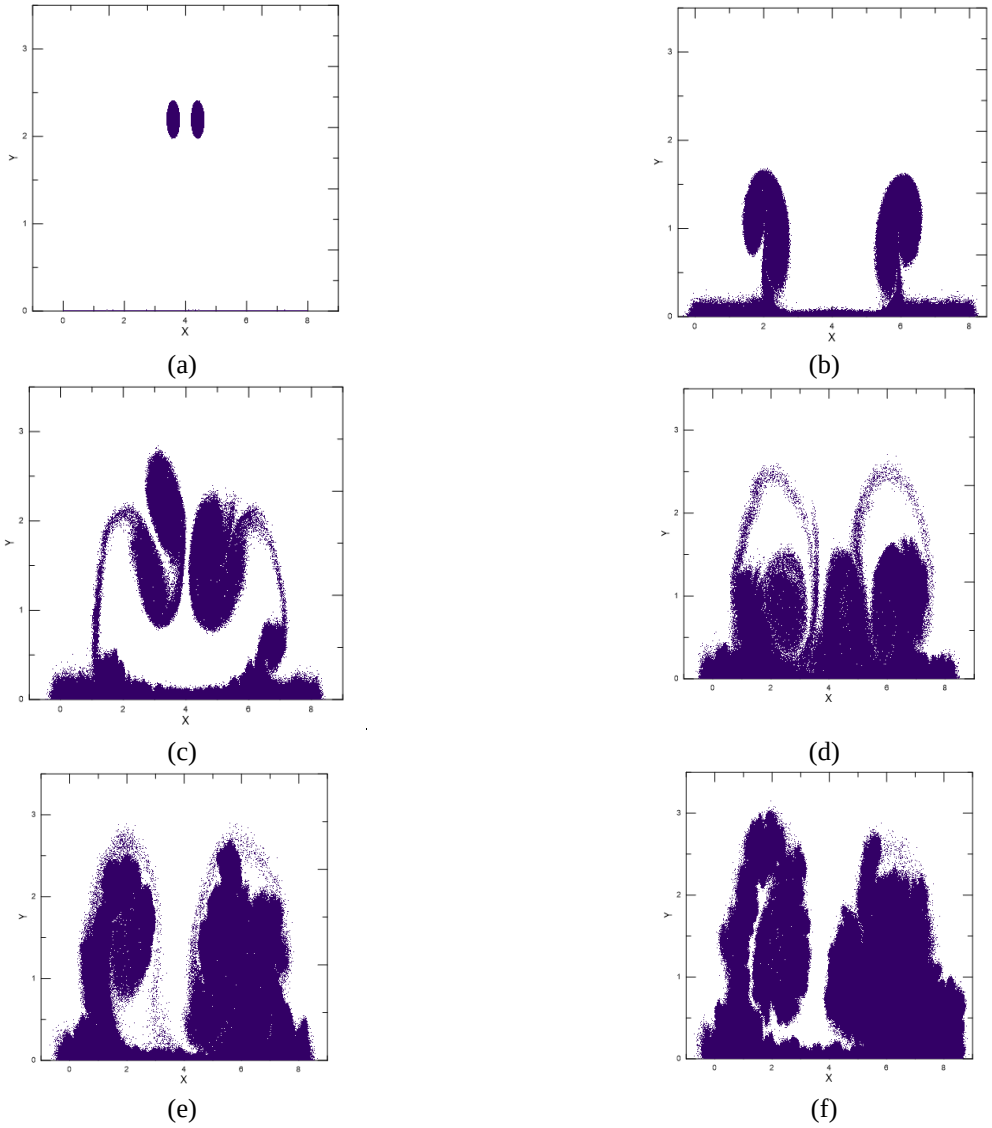

Figure 5. Vorticity field of the simulation (vii) in different time steps. (Euler; $\Delta t = 0.05$; $p = 25$; $nz = 2.5 \times 10^4$; $Re = 7.65 \times 10^3$).

5. CONCLUSIONS

An algorithm of the fast multipole method that was based on the work developed by Ricciardi (2016) and recently implemented in the works of Vidille *et al*. (2021) and Vidille *et al.* (2022) is used to make feasible simulations that the amount of particles present in the fluid domain is high. The CPU time decreased at least 86% in comparison with the simulations whereby the velocity field due to the vortex-vortex interaction was calculated only through the Biot-Savart law. According to the results presented, the simulations that the fast multipole method starts to be used later and the lower refinement levels are predominant in most of the simulations have numerical errors lower (simulation vii), because of the high value of the ratio between the number of particles in the domain and the number of boxes in the maximum refinement level. It is still necessary to study more and run more simulations to obtain the best ratio between the number of particles in the domain and the number of square boxes used in the FMM, i.e., the refinement level. Besides that, it is so important to determine the best step to start using the fast multipole method, and the appropriate moment to execute a domain refinement, reducing the CPU time and the numerical errors associated with the accelerated algorithm.

It is possible, from the present work, to develop research in order to evaluate the behavior of the counterrotating pair of vortices detached from airplane wings using the core spreading method (Rossi, 1996), in order to evaluate if the results obtained using the core spreading method to simulate the vorticity diffusion are closer to the experimental results than that obtained using the random walk method. Furthermore, the use of the core spreading method to solve the diffusion step will avoid the difference between the right and left sides of the discrete vortices cloud, turning these mirrored, what makes the simulation closer to the reality. The obstacle to using this method is the increase in the number of particles in the computational domain during the simulations. It is because of this that the use of the fast multipole method is essential:

if the accelerator algorithm is successfully implemented, it is possible to simulate complex situations, with a higher number of discrete vortices in the domain, in shorter CPU times.

6. ACKNOWLEDGEMENTS

The authors would like to acknowledge São Paulo Research Foundation (FAPESP), grant 2022/03630-4, and Coordenação de Aperfeiçoamento de Pessoal de Nível Superior - Brasil (CAPES), grant 88887.690941/2022-00.

7. REFERENCES

Alcântara Pereira, L. A., 1999. *Simulação numérica do escoamento em torno de um corpo de forma arbitrária utilizando o método de vórtices discretos*. Master Thesis, Federal University of Itajubá.

Alcântara Pereira, L.A., Hirata, M.H. and Manzanares Filho, N., 2004. "Wake and Aerodynamics Loads in Multiple Bodies - Application to Turbomachinery Blade Rows". *J. Wind Eng. Ind Aerodyn*., Vol. 92, pp. 477-491.

Batchelor, G. K., 1967. *An introduction to fluid dynamics*. Nova Delhi: Cambridge University Press.

Bimbato, A.M., Alcântara Pereira, L.A. and Hirata, M.H., 2018. "Development of a new Lagrangian vortex method for evaluating effects of surfaces roughness". *European Journal of Mechanics B-Fluids*, Vol. 74, pp. 291-301.

Chorin, A.J., 1973. "Numerical Study of Slightly Viscous Flow". *Journal of Fluid Mechanics*, Vol. 57, pp. 785-796.

Cipra, B.A., 2000. "The best of the 20th century: Editors name top 10 algorithms". *SIAM News*, Vol. 33, pp. 1–2.

Greengard, L. and Rokhlin, V., 1987. "A fast algorithm for particle simulations". *Journal of Computational Physics*, Vol. 73, pp. 325–348.

Katz, J. and Plotkin, A., 1991. *Low speed aerodynamics: from wing theory to panel methods*. McGraw Hill Inc..

Komoutsakos, P. D., 1993. *Direct numerical simulations of unsteady separated flows using vortex methods*. Thesis (Ph.D.) - California Institute of Technology.

Lewis, R.I., 1991. *Vortex element method for fluid dynamic analysis of engineering systems.* Cambridge Univ. Press, Cambridge, England, U.K.

Lewis, R.I., 1999. "Vortex Element Methods, the Most Natural Approach to Flow Simulation - A Review of Methodology with Applications". In *Proceedings of 1st Int. Conference on Vortex Methods*. Kobe, Japan.

Machol, R., 1993. "Wake Vortices – A Primer*". FAA Aviation Safety Journal*, Vol. 3, No. 1, pp. 16-19.

Nishimura, N., 2002. "Fast multipole accelerated boundary integral equation methods". *Applied Mechanics Reviews*, Vol. 55, pp. 299–324.

Ricciardi, T.R., 2016. *Fast multipole discrete vortex method applied to unsteady flow simulations*. M.Sc. Dissertation, University of Campinas.

Ricciardi, T.R., Wolf, W.R. and Bimbato, A.M., 2017a. "A fast algorithm for simulation of periodic flows using discrete vortex particles". *Journal of the Brazilian Society of Mechanical Sciences and Engineering*, Vol. 39, pp. 45-55.

Ricciardi, T.R., Wolf, W.R. and Bimbato, A.M., 2017b. "Fast multipole method applied to Lagrangian simulations of vortical flows". *Communications in Nonlinear Science and Numerical Simulation*, Vol. 51, pp. 180-197.

Rossi, L.F., 1996. "Resurrecting Core Spreading Vortex Methods: A New Scheme that is both Deterministic and Convergent". *SIAM J. Sci. Comput*., Vol. 17, No. 2, pp. 370-397.

Vidille, M.F., Alcântara Pereira, L.A. and Bimbato, A.M., 2021. "Implementation of an accelerator algorithm to reduce the computational costs in Lagrangian simulations" *In Proceedings of the 26nd International Congress of Mechanical Engineering - COBEM 2021*. Florianópolis, Brazil.

Vidille, M.F., Moraes, P. G., Alcântara Pereira, L.A. and Bimbato, A.M., 2022. "Use of a fast multipole method to reduce the computational costs of aircraft wakes simulations" *In Proceedings of the 19th Brazilian Congress of Thermal Sciences and Engineering – ENCIT 2022*. Bento Gonçalves, Brazil.

Zheng, Z.C. and Ash, R.L., 1996. "Study of Aircraft Wake Vortex Behavior Near the Ground". *AIAA Journal*, Vol. 34, No. 3, pp. 580-588.

8. RESPONSIBILITY NOTICE

The authors are the only responsible for the printed material included in this paper.